Published in final edited form as:
J Comp Neurol. 2010 September 15; 518(18): 3645–3661. doi:10.1002/cne.22445.

Molecular regulation of the developing commissural plate

Randal X. Moldrich[1], **Ilan Gobius**[1], **Thomas Pollak**[1], **Jiangyang Zhang**[3], **Tianbo Ren**[1], **Lucia Brown**[4], **Susumu Mori**[3,5], **Camino de Juan**[6], **Olga Britanova**[6], **Victor Tarabykin**[6], and **Linda J. Richards**[1,2]

[1] The University of Queensland, The Queensland Brain Institute, Brisbane, QLD 4072, Australia

[2] The University of Queensland, The School of Biomedical Sciences, Brisbane, QLD 4072, Australia

[3] Division of NMR Research, Department of Radiology, Johns Hopkins University School of Medicine, Baltimore, Maryland 21205, USA

[4] Department of Obstetrics, University of Vermont, Gynecology and Reproductive Sciences, Burlington, Vermont 05401, USA

[5] F.M. Kirby Functional Imaging Center, Kennedy Krieger Institute, Baltimore, Maryland, 21205, USA

[6] Max-Planck-Institute for Experimental Medicine, 37075 and the Research Center for the Molecular Physiology of the Brain (CMPB), 37073 Gottingen, Germany

Abstract

Coordinated transfer of information between the brain hemispheres is essential for function and occurs via three axonal commissures in the telencephalon: the corpus callosum (CC), hippocampal commissure (HC) and anterior commissure (AC). Commissural malformations occur in over 50 human congenital syndromes causing mild to severe cognitive impairment. Disruption of multiple commissures in some syndromes suggests that common mechanisms may underpin their development. Diffusion tensor magnetic resonance imaging revealed that forebrain commissures crossed the midline in a highly specific manner within an oblique plane of tissue, referred to as the commissural plate. This specific anatomical positioning suggests that correct patterning of the commissural plate may influence forebrain commissure formation. No analysis of the molecular specification of the commissural plate has been performed in any species, therefore we utilized specific transcription factor markers to delineate the commissural plate, and identify its various sub-domains. We found that the mouse commissural plate consists of four domains, and tested the hypothesis that disruption of these domains might affect commissure formation. Disruption of the dorsal domains occurred in strains with commissural defects such as *Emx2* and *Nfia* knockout mice but commissural plate patterning was normal in other acallosal strains such as *Satb2*. Finally, we demonstrate an essential role for the morphogen, *Fgf8* in establishing the commissural plate at later developmental stages. The results demonstrate that correct patterning of the commissural plate is an important mechanism in forebrain commissure formation.

Keywords

Commissural plate; Nuclear factor I (Nfi); Empty spiracles homeobox (Emx); Sine oculis-related homeobox 3 homolog (Six3); Zinc finger protein of the cerebellum 2 (Zic2); Fibroblast growth factor 8 (Fgf8)

Author for correspondence: Prof. Linda J. Richards, The Queensland Brain Institute, The University of Queensland, Brisbane, Queensland, 4072 Australia. Ph: 61 7 3365 2661, Fax: 61 7 3365 1299, richards@uq.edu.au.

Introduction

Early anatomical studies described a unique anatomical region within the brains of many mammalian species, where all telencephalic commissures initially cross the interhemispheric midline; this region was termed the commissural plate (Rakic and Yakovlev, 1968 and references therein). Rakic and Yakovlev (1968) proposed that the human commissural plate could be anatomically divided into dorsal and ventral domains, respectively termed the massa commissuralis (MC) where the corpus callosum (CC) and hippocampal commissure (HC) cross, and the area septalis (or septal area, SA), where the anterior commissure (AC) crosses the midline. To date, there has been no anatomical characterization of the commissural plate in the mouse, nor any molecular characterization in any species.

During early embryogenesis, patterning centers of morphogens such as fibroblast growth factors (*Fgf*), sonic hedgehog, bone morphogenic proteins and the secreted Wnt proteins divide the brain into various sectors (Hebert, 2005; Takahashi and Liu, 2006), including the pallium and the subpallium (Rubenstein et al., 1998). One such forebrain patterning center is the commissural plate, which expresses *Fgf8* (Shimamura and Rubenstein, 1997; Fukuchi-Shimogori and Grove, 2001; Shimogori et al., 2004; Storm et al., 2006) and patterns the cerebral cortex into functionally specific domains (O'Leary and Sahara, 2008). Although the commissural plate has been identified as an early patterning center, it is not clear whether this region corresponds to that described by Rakic and Yakovlev (1968) as the area where all forebrain commissures cross the midline. A more detailed analysis of this region throughout development is required to connect the two developmental functions of the commissural plate, namely patterning and commissure formation.

To examine the development of all midline commissures in the same brain in three dimensions we used diffusion tensor magnetic resonance imaging (DTMRI), which measures the direction and microstructural properties of white matter tracts. DTMRI was used to virtually section the embryonic brain at any angle, revealing that the three commissures formed initially within a single oblique coronal plane of tissue, which we could then section histologically at the same angle. This allowed us to observe this "plate" of tissue in a single section and to identify molecular expression domains that could delineate each region of the commissural plate. Transcription factors and anatomical correlates were used to define four domains of the mouse commissural plate. These included the nuclear factor I family (*Nfia*), empty spiracles homologs (*Emx1*), sine oculis-related homeobox 3 (*Six3*) and the zinc finger protein of the cerebellum 2 (*Zic2*) (Yoshida et al., 1997; Ogura et al., 2001; Shu et al., 2003; Steele-Perkins et al., 2005; Lavado et al., 2008). Patterning of these domains was disrupted in mice with commissural defects and deficient in NFIA and EMX2 proteins. However, patterning was not disrupted in the *Satb2* knockout mice, which also displays commissural defects. Finally, we found that *Fgf8* is required for patterning the dorsal domains of the commissural plate. Overall, this analysis establishes a framework for understanding the development of this important brain region and its role in commissure formation.

Materials and Methods

Animals

Wildtype C57Bl/6J, and litters of *Emx2* (Pellegrini et al., 1996), *Nfia* knockout mice (Steele-Perkins et al., 2005) and $Fgf8^{flox/flox}$ (Meyers et al., 1998) crossed with $Emx1^{Cre}$ (Iwasato et al., 2004) animals, were bred on site at the University of Queensland under approval from the institutional Animal Ethics Committee. Mice knockout for the special AT-rich sequence binding protein 2 (*Satb2*; Britanova et al., 2006) were maintained at the Max-Planck-

Institute for Experimental Medicine in accordance with German law and approved by the Bezirksregierung Braunschweig; the brains were shipped to the University of Queensland for experimental analysis. Targeted deletion of *Fgf8* in the dorsal forebrain was performed by crossing the *Fgf8*$^{flox/flox}$ and *Emx1*^{Cre} strains (both conditional alleles with wildtype activity) to generate *Emx1-cre;Fgf8*$^{flox/flox}$ mice. Mapping *Emx1* Cre recombinase in the cortex was performed by crossing *Emx1*^{Cre} mice with those expressing green fluorescent protein (GFP) following loxP recombination (B6;129-*Gt(ROSA)26Sor*^{tm2Sho}/J known here are ROSA26-eGFP^{flox} (Mao et al., 2001)). Transgenes used to produce the genetically modified mice are detailed in Table 1. Timed-pregnant dams were identified by the presence of a vaginal plug, this being designated as embryonic day 0. Embryos were genotyped by PCR as previously described for the *Nfia*$^{-/-}$ (Steele-Perkins et al., 2005), *Emx2*$^{-/-}$ (Pellegrini et al., 1996), *Fgf8*$^{flox/flox}$ (Meyers et al., 1998), *Emx1*^{Cre} (Iwasato et al., 2004), ROSA26-eGFP^{flox} (according to The Jackson Laboratory genotyping protocol for this strain) and *Satb2*$^{--}$ strains (Britanova et al., 2006). For embryo perfusion, pregnant dams at the appropriate gestational stages were first deeply anesthetized (6.5 mg/ml sodium pentobarbitone, i.p.) and embryos recovered by cesarian section. Embryonic day 14 (E14) heads were immersion fixed in 4% w/v paraformaldehyde (PFA; ProSciTech, Australia) in phosphate buffered solution (PBS; pH 7.4; Lonza, USA). Embryos from stages E15 to E17 were transcardially perfused using 0.9% saline solution (0.9% w/v NaCl in double-distilled H_2O) for 2 min, followed by 4% PFA for 4 min. At least three animals were used per experiment.

Diffusion tensor magnetic resonance imaging (DTMRI)

Imaging of E14 to E17 C57Bl/6 brains (in heads) was performed using an 11.7 Tesla magnetic resonance spectrometer (Biospin; Bruker, Billerica, MA) following incubation in 1 μM Magnevist (Berlex Imaging, USA). Diffusion-weighted (DW) images were acquired with a three-dimensional DW fast spin echo sequence (Mori and van Zijl, 1998) as previously described (Ren et al., 2007). Briefly, the imaging involved a repetition time of 700 ms, echo time of 27 ms, imaging resolution of 0.09 × 0.09 × 0.09 mm, signal averages of 4, and twin navigator echoes for eddy current correction. Two non-DW images and six DW images (b = 1200 s/mm^2) were acquired. The total imaging time was approximately 15 h. The diffusion tensor was calculated using a log-linear fitting method, with three pairs of eigenvalues and eigenvectors calculated for each pixel. The eigenvector associated with the largest eigenvalue was referred to as the primary eigenvector. Files were reassembled using DTI-Studio (www.mristudio.org) and color maps were generated using fractional anisotropy and primary eigenvector analyzes. An angle of zero degrees for calculation of the oblique coronal plane was taken from the base of the brain along the ventral hypothalamus. Tractography was performed using DTI-Studio.

Antibodies

Antibodies, sources and their concentrations are shown in Table 2.

The GAP-43 (Clone 9-1E12; Chemicon; MAB347) antibody specifically detects a single band in Western blots at ~45kDa on rat brain and nerve tissues (Schreyer and Skene, 1991) and on mouse brain extracts and mouse brain membrane fractions of growing neurons (manufacturer's information).

The NFIA antibody was purchased from Active Motif (39329) and used at 1:1000. The specificity of anti-NFIA in the mouse has been previously confirmed by Western blot analysis with HA-tagged NFIA, peptide blocking experiments and using *Nfia* knockout mice (Plachez et al., 2008).

Anti-GFP is a rabbit polyclonal IgG antibody raised against GFP that was isolated directly from *A. victoria* and purified by ion-exchange (manufacturer's information). Specificity of the antibody was confirmed in the present study by immunohistochemistry (1:1000) in a non-GFP-expressing mouse line (C57Bl/6; data not shown) and in a GFP-expressing mouse line (Emx1cre-ROSA26; see Results section).

Rabbit anti-glial fibrillary acidic protein (GFAP) IgG (Dako, USA; Z0334) was produced from purified bovine spinal cord isolate (manufacturer's information). Specificity of this antibody in mouse brain has been confirmed by immunohistochemistry in GFAP knockout mice (Hanbury et al., 2003).

The rabbit anti-ZIC2 antibody was produced by Brown et al. (2003) using the protein produced from a cloned human *ZIC2* fragment that corresponded to amino acids 2-109. The anti-serum was reactive by immunohistochemical and immunoblot methods only in CHO cells transfected with *Zic2* at the expected 55kDa weight, but not *Zic1* or *Zic3* expression plasmids. As expected, immunoreactivity was localised to the nucleus in cultured CHO cells (Brown et al., 2003).

The rabbit anti-EMX1 antibody was produced from recombinant human EMX1 and characterized by Briata et al. (1996). In that study, the antiserum identified a single band corresponding to EMXl (31 kDa) in protein extracted from E13.5 mouse telencephalon, and a single ~31kDa band from Sf9 cells expressing EMX1, but not EMX2, in which no band was observed. During this characterization the preadsorption control produced no staining. A Western blot of total lysates of the telencephalon of an E13.5 and a new-born mouse reacted with the EMX2-adsorbed anti-EMXl antiserum revealing a single ~31kDa band.

A synthetic peptide corresponding to amino acids 270–289 of the mouse SIX3 protein (GenBank AAH94426) was used as the antigen to produce the protein A-purified polyclonal antibody in guinea pigs (Rockland Immunochemicals, USA; 200-201-A26). Titration experiments at concentrations between 1:100 and 1:1000 revealed optimal immunoreactivity at 1:200. Preadsorption control immunohistochemistry was performed using the synthetic peptide at 50× the antibody concentration (Supp. Fig. 1), and revealed selective immunoreactivity in the mouse E17 forebrain, corresponding to known *Six3* expression (Oliver et al., 1995).

Goat, affinity-purified fluorescent secondary antibodies included anti-mouse Alexa Fluor 633 (1:100; A21126, Invitrogen, Australia), anti-rabbit Alexa Fluor 488 (1:200; A11034, Invitrogen, Australia) and anti-guinea pig Alexa Fluor 546 (1:200; A11074, Invitrogen, Australia). Additional chromogenic immunohistochemistry was performed for GAP43 (as above) with donkey anti-mouse biotin-SP-conjugated secondary antibody (715-065-150, Jackson ImmunoResearch Laboratories, USA), and for rabbit anti-GFP (A11122, Invitrogen, Australia) using goat anti-rabbit biotin-conjugated secondary antibody (BA-1000, Vector laboratories, USA).

Immunohistochemistry and image acquisition

Paraffin tissue infiltration and paraffin-embedded sectioning were utilized to obtain 5 μm sections. As DTMRI revealed the commissural plate to be an oblique structure, we developed a technique to obtain sections spanning the commissural plate at the oblique coronal orientation as well as in a standard sagittal plane. This novel sectioning angle was achieved by melting paraffin-embedded tissue blocks onto an angled wooden chuck to achieve an oblique complementary cutting angle. Sections were deparaffinized and rehydrated with a series of xylene and ethanol washes. Antigen retrieval was performed under pressurized heat in sodium citrate buffer (10mM $C_6H_5Na_3O_7$. $2H_2O$, 0.05% v/v

Tween 20 in MilliQ™ H_2O, pH 6.0) using an antigen de-cloaking chamber (Biocare Medical, USA). Following antigen retrieval, all steps were performed in 0.0025% v/v Triton X-100 and PBS. Immunofluorescence analysis was performed following 10% normal goat serum blocking. Primary antibodies were incubated overnight at 4°C, followed by repeated washes and secondary antibody incubation for 2 h at room temperature. All sections were also stained for the nuclear marker DAPI (1:1000) (Invitrogen, Australia). Sections were coverslipped in PVA/DABCO mounting medium (Sigma-Aldrich, Australia). Immunofluorescence analysis was performed such that GAP43, SIX3 and ZIC2 were revealed on the same section (as described above), with EMX1 and NFIA (each with GAP43) immunohistochemistry performed on the preceding and following serial section, allowing overlay of images. Chromogenic immunohistochemistry was performed using avidin-biotin amplification (PK-6100, Vector laboratories, USA) and 3,3′-diaminobenzidine (DAB; Sigma-Aldrich, Australia) visualization. Bright field imaging and fluorescence imaging were performed with a Zeiss upright Axio-Imager Z1 microscope fitted with AxioCam HRc and HRm cameras. Images were pseudocolored to permit overlay, cropped, sized and brightness-enhanced for presentation with Adode Photoshop.

In situ hybridization

For *in situ* hybridization, embryos were transcardially perfused with 4% PFA and vibratome sectioned at 45μm. Sections were then mounted onto Superfrost slides (Menzel-Glaser, Brunswick, Germany) and allowed to dry. Sections were fixed with 4% PFA, permeablised with Proteinase K (10μm/mL in PBS; Roche, Mannheim, Germany), re-fixed with 4% PFA, followed by acetylation in a solution of 1.33% triethanolamine, 0.064% hydrochloric acid, and 0.375% acetic anhydride. All hybridizations were performed at 68°C overnight. Sense and antisense riboprobes were generated for a 266bp sequence extending from 20bp 3′ of exon 2 to the stop codon in exon 3 (courtesy of Prof Gail Martin, UCSF, USA). Probes were digoxigenin-labeled (DIG RNA Labeling Mix; Roche, Mannheim, Germany), detected with anti-digoxigenin-AP at 1:4000 (Roche, Mannheim, Germany), and visualized with the color substrate BM Purple (Roche, Mannheim, Germany).

Measurements and statistical analysis

Oblique coronal angles were determined using exported DICOM sections from DTI-Studio and ImageJ software. Measurements of anatomical and molecular domains were taken from the AC (point zero) using ImageJ software. Graphs were prepared of the mean ± S.D. using GraphPad Prism v.4 (GraphPad Software, USA). Wildtype littermates served as controls for the knockout mice and all controls were pooled for graphical representation. All experimental procedures were performed on at least three individual mice of each genotype. Statistical differences between conditions were established using two-way ANOVA with Bonferroni's post-hoc t-test whereby $p < 0.05$ (GraphPad Prism v.4).

Results

DTMRI reveals that all commissures cross the midline in a common oblique-coronal plane

Investigating the embryonic development of multiple axon tracts in the same brain has previously proven challenging. Live tract-tracing techniques, and even tract-tracing in fixed tissue using carbocyanine dyes, do not allow the unbiased labeling of all axons comprising a single tract, due to the nature of the dye or tracer placement (usually at a single injection site). Moreover, multiple injections of different tracts in a single brain are difficult to perform and to analyze in three-dimensions. We wanted to examine the development of the AC, HC and CC in the same brain to gain an understanding of how these tracts develop in relation to one another and to determine where they first cross the midline. To do this, we used DTMRI to generate a three-dimensional map of the fiber tracts and their orientation

(Fig. 1). DTMRI, which can be used on fixed (or living) brains, analyzes the diffusion of water-molecules along ordered structures in the brain. The orientation of this diffusion can then be color-coded to provide a color-map in three dimensions of all the fiber tracts in the brain. Color orientation maps were generated from fractional anisotropy calculations and primary eigenvector maps using DTI-Studio. The advantage of this approach is that imaging data can be viewed in any plane of optical section, providing novel ways of looking at how multiple fiber tracts develop in relation to one another. As previously described, the AC was the first forebrain commissure to cross the midline and is visible by DTMRI at E14 (Fig. 1A). At E15, the HC was similarly identified both dorsal and rostral to the AC (Fig. 1B). At E15, both commissures crossed the midline at an oblique coronal angle of approximately −58° to the base of the brain. The AC and HC increased in size in the sagittal plane (Fig. 1C) at E16, but with brain growth they now crossed at an angle of approximately −65° to the ventral surface of the brain. Although CC axons are known to cross at this stage (Rash and Richards, 2001), they either could not be detected at the current imaging resolution or could not be distinguished from the HC axons by DTMRI until E17 (Fig. 1D). The CC then extended rostrally. At E17, the AC, HC and caudal extent of the CC formed an angle of −68° to the ventral surface of the brain, or 22° from the traditional coronal plane. Therefore, the oblique angle of the commissural plate became increasingly obtuse during embryonic development to reach −68° at E17, at which stage all three forebrain commissures had crossed the midline.

A comparison of traditional coronal images (Figs. 1A′-D′) and oblique coronal images (Figs. 1A″-D″) demonstrated that the commissures crossed within a single plane of tissue, not visible in traditional coronal sections. This single plane of tissue is the commissural plate.

Analysis of commissural tracts within the commissural plate

To further validate the identification of the commissural plate by DTMRI, we performed a histological analysis at E17, when each forebrain commissure could be identified as a substantial tract. A detailed anatomical analysis of all forebrain commissures in the oblique plane was also necessary in order to identify how different regions of the commissural plate related to the different commissural projections. Paraffin-embedded tissue sections at 5 μm were stained with anti-GAP43 to identify axon tracts (Shen et al., 2002). Sectioning the brain at an oblique coronal angle (68°) allowed the full dorsoventral axis of the commissural plate, including all forebrain commissures, to be viewed in a single section, which was not possible by sectioning in the traditional coronal plane.

The rostral commissural plate was dominated by the CC (Fig. 2C), which crosses the midline at the boundary between the cingulate cortex and septum. More caudally however, the CC, HC and AC crossed the midline at an oblique angle of 68° (Figs 2D, E). Moreover, two distinct components of the HC could be easily observed: the dorsal HC (DHC) and the ventral HC (VHC). Further ventrally, axons forming the dorsal columns of the fornix (DCF) were apparent (Fig. 2F′), dorsal to the AC.

The commissural plate consists of multiple molecular domains

The anatomy of the commissural plate had previously been described in human fetal brain (Rakic and Yakovlev, 1968) as having dorsal and ventral domains, but nothing was known about the molecules expressed in these domains. To begin to address this, we first investigated the expression of genes at E17, in relation to where the different forebrain commissures formed. A dorsal MC domain and a ventral SA domain were tentatively designated in the mouse according to the anatomical model originally proposed for the human commissural plate (Rakic and Yakovlev, 1968). By screening known candidate genes we determined that the MC could be identified by the expression of the pallial markers

NFIA (Plachez et al., 2008) and EMX1 (Boncinelli et al., 1993). The ventral SA could be identified by the subpallial markers SIX3 (Oliver et al., 1995) and ZIC2 (Brown et al., 2003). Importantly, these markers are expressed early during development and could provide molecular landmarks throughout the embryonic development of the commissural plate.

The pattern of NFIA immunoreactivity followed the ventricular zones of the dorsal and ventral reaches of the lateral ventricles, and was particularly intense ventral to the CC and dorsal to the DHC in the region of the glial wedge (Fig. 3A, B) (Shu et al., 2003). NFIA immunoreactivity was intercalated with the fibers of the DHC, but not in the VHC, and became more dispersed in the septum, ventral to the VHC, and with a few immunoreactive cells present ventral to the AC. In addition, a cluster of NFIA-immunoreactive cells was present dorsal and rostral to the AC as revealed in the sagittal plane (arrow in Fig. 3C), which corresponds to the ventral diagonal band of Broca. NFIA immunoreactivity also bordered the caudal commissural plate, with NFIA being expressed in the epithelium and ventricular zone of the rostral wall of the third ventricle (asterisk in Fig. 3C). EMX1 immunoreactivity was located dorsal and ventral to both the DHC and the CC similar to the pattern seen with NFIA, but did not extend ventrally past the VHC.

Two ventral markers, ZIC2 AND SIX3 were preferentially expressed in the SA. ZIC2 was present around the lateral aspects of the VHC and dorsal to the AC whereas SIX3 expression was more ventral and surrounded the AC. Similar to NFIA, ZIC2 was expressed in the epithelium of the rostral wall of the third ventricle between the commissural plate and the diencephalon (Fig. 3D). This expression analysis demonstrated that EMX1 and NFIA were expressed in the MC, but NFIA was also expressed in the dorsal SA (designated SA_1). ZIC2 expression overlapped with that of NFIA in the ventral MC (MC_2), and overlapped with NFIA and SIX3 expression in the dorsal SA (SA_1). Only SIX3 was expressed in the ventral SA (designated SA_2).

In summary, based on the above data, the mouse commissural plate can be divided more usefully into four molecular domains, each associated with a specific commissural projection. From dorsal to ventral these are: MC_1, associated with the CC labeled with NFIA and $EMX1^+$; MC_2, associated with the DHC and VHC labeled with $NFIA^+$, $EMX1^+$ and $ZIC2^+$; SA_1, associated with the fornix labeled with $NFIA^+$, $ZIC2^+$ and $SIX3^+$; and SA_2, associated with the AC labeled with $SIX3^+$ (summarized in Fig. 10). Since NFIA and EMX1 overlapped in the MC, either could be used to label this region.

Molecular development of the commissural plate

Having established the basic expression of genes in different domains within the commissural plate, we wanted to investigate earlier developmental stages to determine if these markers defined the different regions of the commissural plate before, and during, the time at which the first commissural axons cross the midline. This information would be useful in determining whether commissural plate formation could play an instructive role in commissure development and positioning. A series of oblique coronal sections of the dorsoventral length of the commissural plate was prepared from E14–E17 brains and fluorescence immunohistochemistry performed (Fig. 4).

At E14 (Fig. 4A–E), the dorsal-most fibers of the fornix converged at the midline within MC_2 and passed ventrally through SA_1. Therefore, at E14, the fornix delineates the boundary between the MC and the SA. However, ventrally, ZIC2- and SIX3-positive domains defined a molecular boundary in the SA, delineating SA_1 and SA_2 respectively, even at this early developmental stage. SIX3 was weakly expressed in the dorsal midline at this age (Fig. 4D).

At E15, a small number of callosal pioneering axons projected from the cingulate cortex towards the midline within the dorsal MC_1 (Fig. 4F–J). The HC also crossed the midline within the ventral MC_2 domain. Ventrally, ZIC2 and SIX3 expression continued to define the SA_1 and SA_2 regions, respectively, although the border between these regions was not sharp. Furthermore, the AC crossed the midline within the SIX3-positive domain such that a region of SIX3 expression bordered this commissure later in development (Fig. 4K–T).

Anatomically, the dorsal and ventral components of the HC can be distinguished at E16 and this became important for delineating the domains of the MC. The DHC and VHC crossed the midline within MC_2, whereas the CC crossed within the MC_1. We next addressed whether the delineation of these domains conferred any functional relevance to the formation of the forebrain commissural projections.

Patterning of sub-domains within the commissural plate affects commissure formation

To test the hypothesis that correct commissural plate development may be a requirement for forebrain commissural formation, we analyzed a number of mouse mutants (*Nfia*$^{-/-}$, *Emx2*$^{-/-}$, *Satb2*$^{-/-}$ and *Emx1-cre;Fgf8*$^{flox/flox}$ mice) in which forebrain commissure formation is known to be disrupted, and analyzed the development of the commissural plate in these animals using the markers we had defined above. *Nfia* and *Emx2* knockout mice were chosen because these mice have previously been shown to exhibit defects in midline development (Pelligrini et al., 1996; Shu et al., 2003; Piper et al., 2009), specifically in the size of the cingulate cortex, whose most ventral region comprises part of MC_1. *Fgf8* conditional knockout mice were investigated because *Fgf8* is known to be expressed in the commissural plate, prior to commissure formation, when this region serves as the rostral patterning center (Tole et al., 2006; Cholfin and Rubenstein, 2008). If differences in commissural plate patterning were observed in these mutants we could not be sure whether the commissural plate was disrupted as a consequence of defects in commissure formation. Therefore, as a comparison, we also examined patterning of the commissural plate in a mouse model that displays commissural defects, but contains a mutation for a gene which is not expressed in the septum (the likely main adult derivative of the commissural plate), and is not know to have midline defects. As *Satb2* is expressed within callosal axons and determines their choice of trajectory during development in a cell-autonomous manner (Alcamo et al., 2008; Britanova et al., 2008), in this way analysis of *Satb2* knockout mice served as a comparison for commissural patterning as a result of commissural defects.

To examine commissural plate development, we labeled brains from each mutant strain with the key commissural plate markers EMX1, NFIA, ZIC2 and SIX3. This also allowed us to measure the changes in commissural plate domains in *Nfia* knockout mice and to measure the size of the expression domains in each mutant (as demonstrated in Supp. Fig. 2). Measurements were made using the sagittal plane because, in the absence of commissural projections, it was difficult to identify the exact oblique-coronal plane of tissue for comparison in the absence of the axonal tracts.

Nfia is important for the formation of glial populations at the midline (Shu et al., 2003), and the subsequent development of the CC and HC. Measurements of the commissural plate domains indicated a significant expansion of the MC in *Nfia* knockout mice (Fig. 5F). An increase of approximately 475 μm was observed in the total distance from the AC to the dorsal surface of the brain ($p < 0.001$). Although a reduction in the size of the SA_2 domain was also observed, this was not significantly different from that of wildtype littermates. *Emx2* is a transcription factor required for correct arealization of the cortex (Yoshida et al., 1997; Bishop et al., 2000; Mallamaci et al., 2000) and the formation of commissural projections, as well as the development of the cingulate cortex (Pellegrini et al., 1996; Yoshida et al., 1997). *Emx2*$^{-/-}$ mice displayed a reduction in the size of the MC but a

significant expansion in SA_1 compared with control animals ($p < 0.05$). In *Emx2*$^{-/-}$ mice, the AC is disrupted to varying extents, but exists, thus allowing measurement of the commissural plate domains using the AC as a reference point. As illustrated in Fig. 5C, the AC of *Emx2*$^{-/-}$ mice was thin and defasciculated. These results demonstrate that either an expansion or a reduction in the size of the MC is correlated with defects in CC and HC formation, and that an expansion of the SA_2 domain may affect AC development.

Thus far, our results had correlated disruptions in commissural projections with disruptions in commissural plate domains. However, it is possible that defects in the size of commissural plate domains occur as a consequence of the lack of formation of commissural projections. One argument against this is that we based our analyses on differences in protein expression domains and not differences in axonal projections. However, to address this issue further we analyzed the size of the commissural plate domains in *Satb2* knockout mice, which display commissural defects through the cell-autonomous regulation of cortical lamination and axonal targeting, rather than the regulation of the development of the midline.

SATB2 is a chromatin remodeling protein that regulates commissural neuron identity in the neocortex (Britanova et al., 2008; Gyorgy et al., 2008). As *Satb2*$^{-/-}$ mice have agenesis of the CC, a larger AC and a thinner cortex, we reasoned that there may be a change in the size of the MC. Unlike *Nfia* and *Emx2*, the absence of *Satb2* had no effect on the sizes of the expression domains of EMX1/NFIA or SIX3 (Fig. 5D), despite the mutants having no CC and a larger AC. There was a slight dorsal expansion of the expression domain of ZIC2 due to the absence of the CC. To further investigate midline development in the *Satb2*$^{-/-}$ mice we stained oblique coronal sections with GFAP to label midline glial populations. Three such populations were present at the midline, the glial wedge, the indusium griseum glia (IGG) and the midline zipper glia (MZG) (Fig. 6A). The only difference from control brains was that the IGG and MZG had not been split by the formation of the CC (Fig. 6B), thus *Satb2*$^{-/-}$ mice display normal development of the commissural plate and the midline glial structures associated with it, despite their midline commissural defects. This phenotype demonstrates that disruptions in commissural projections do not affect the gross size of the commissural plate domains *per se* and instead supports the hypothesis that the correct patterning of the commissural plate is a mechanism regulating forebrain commissure formation.

Fgf8 is required for formation of the commissural plate

Fgf8 is expressed in the rostral patterning center during early embryogenesis (Maruoka et al., 1998), and later at the midline within the presumptive commissural plate (Crossley and Martin, 1995; Yaylaoglu et al., 2005). *In situ* hybridization for *Fgf8* demonstrated that *Fgf8* mRNA expression was confined to the border between the broader MC and SA domains in the MC_2 and SA_1 domains of the commissural plate (Fig. 7). Since knockout of *Fgf8* results in early embryonic lethality and gross telencephalic dysmorphology, conditional knockout lines have been generated to study middle to late embryonic development (Meyers et al., 1998). Similarly, conditional knockout lines for Fgf receptor 1 (*Fgfr1*) used to study brain development have identified that this receptor participates in midline and commissural defects later in development (Smith et al., 2006; Tole et al 2006). Here, we used a Cre/loxP recombinase system to remove *Fgf8* (Meyers et al., 1998) in the CoP following activation of the *Emx1* promoter (Iwasato et al., 2004) (Fig. 7). This conditional knockout activity is expected to occur from E10.5 when both *Fgf8* and *Emx1* are expressed in the most rostral aspect of the forebrain (see Iwasato et al., 2004 and Kawauchi et al., 2005). Successful targetting of the Cre/loxP system is demonstrated in Fig. 7 at E14. In *Emx1-cre;Fgf8*$^{flox/flox}$ mutants, *Fgf8* is absent from the commissural plate (Fig. 7F), compared to controls (Fig. 7D). *Emx1-cre;Fgf8*$^{flox/flox}$ embryos developed throughout gestation but did not survive

postnatally. At E14, mutants exhibited hypoplasia of the olfactory bulbs and loss of the septum (Fig. 8), as previously described for *Foxg1-cre;Fgfr1* mutants (Tole et al., 2006). At E18, communication between the lateral ventricles was evident in the *Emx1-cre;Fgf8*$^{flox/flox}$ mutant due to the lack of septum development (Fig. 8H). Furthermore, as described for *Fgfr1* mutants, *Emx1-cre;Fgf8*$^{flox/flox}$ mutants displayed agenesis of the CC and HC (Fig. 8J–L). Dysgenesis of the AC was apparent in some embryos, although AC midline crossing remained (Fig. 8L). In addition to the structural MRI images, hematoxylin staining demonstrated a loss of almost the entire commissural plate, with the exception of the caudal MC_1 domain (Fig. 8J-J′). In this region, some tissue remained and cortical axons approached, but did not cross the midline (Fig. 8L-L′). The hippocampus was slightly smaller than control (data not shown). Only a few fimbria glia were present in *Emx1-cre;Fgf8*$^{flox/flox}$ mutants (Fig. 8K-K′). Axonal tractography of the corpus callosum in *Emx1-cre;Fgf8*$^{flox/flox}$ mutants demonstrated that callosal axons grew in a rostro-caudal trajectory, rather than a medio-lateral trajectory (Fig. 9). Although NFIA, SIX3, EMX1 and ZIC2 expression remained where tissue was present (Fig. 8M–P), the dramatic phenotype meant that no measurements of the medial commissural plate subdomains were possible, hence demonstrating an absolute requirement for FGF8 in formation of the commissural plate.

Discussion

The current investigation characterized the mouse commissural plate as an oblique plane of tissue, within which all telencephalic commissures cross the midline into the contralateral hemisphere during embryonic development. This morphology is generally consistent with earlier histological studies of commissural plate anatomy in other mammals, including humans (Mihalkovics, 1877; Zuckerkandl, 1901; Hochstetter, 1929; Abbie, 1940; Rakic and Yakovlev, 1968). A significant advance in the analysis here is that we have used specific gene expression domains, as well as the dorso-ventral position of the three forebrain commissural projections, to identify that, at least in mouse, there are four, rather than two, distinct domains within the commissural plate. These expression domains are not abrupt, but rather, form gradients whereby either alone or in combination with another gene they become predominant occupiers of the CoP along its dorso-ventral aspect. In addition, anatomical correlations can be used to delineate different areas of the commissural plate. We have described how the MC_1 is associated with the CC and DHC, the MC_2 is associated with the VHC, the SA_1 is associated with the fornix and the SA_2 is associated with the AC. Although the molecular specification of the human commissural plate has not been investigated, species differences in the regions of the commissural plate may arise because of the notable presence of both a dorsal and ventral HC in mice, whereas in humans, the VHC is reduced to such an extent that its existence is questionable (Gloor et al., 1993). One probable reason for this species difference is that, in mouse, we have shown that the VHC lies in the MC_2, a region comprising the ZIC2-immunopositive septum, and that relatively, the septum is much larger in the mouse than the human septum pellucidum. Therefore, the MC_2 may be unique to the mouse brain commissural plate. In future, our analysis in mouse could be used to determine the molecular domains of the human commissural plate.

Nevertheless, the results demonstrate that there are four distinct domains in the mouse based on the protein expression of one, two, or three of the markers used (NFIA, EMX1, ZIC2 and SIX3) (Fig. 10). Our results therefore provide a method for understanding and analyzing the development of this region of the brain and how these domains regulate the crossing and dorso-ventral positioning of different forebrain commissural projections.

Having established that distinct molecular domains exist within the commissural plate, we investigated whether these genes regulate the size of the different commissural plate domains by examining commissural plate development in mouse mutants of four different

genes, *Nfia*, *Emx2*, *Fgf8* and *Satb2*. *Nfia* and *Emx2* knockout mice were predicted to display defects in the MC based on previous work indicating an expansion or loss of the cingulate cortex respectively (Pellegrini et al., 1996; Shu et al., 2003; Piper et al., 2009), part of which makes up the MC_1 domain. This was indeed the case, although in the case of *Emx2*, despite a tendency towards a smaller MC, our measurements did not reach statistical significance. However, we did find a statistically significant expansion of the SA domain labeled by ZIC2. Given that *Emx2* is not expressed in the subpallium, this result indicates that *Emx2* might normally restrict the size of the SA through as yet unidentified mechanisms. In contrast, NFIA deficient mice displayed an overall expansion in the size of the dorso-ventral midline. The *Nfia* mutation caused an expansion of the MC domain without causing an increase in the SA domains, indicating that *Nfia* may normally regulate the size of the MC through proliferation and/or differentiation.

To examine whether these differences in commissural plate domains were meaningful in terms of providing a mechanistic requirement for commissure formation, we utilized the *Satb2* knockout (Britanova et al., 2006), where commissural projections are disrupted without the gene being expressed within the septum (Alcamo et al., 2008; Britanova et al., 2008). Disruption of callosal neuron identity by knockdown of *Satb2* has been reported to affect neocortical thickness and to cause severe CC dysgenesis and misrouting of cortical axons towards the AC and corticospinal tract (Alcamo et al., 2008; Britanova et al., 2008). In the present study, $Satb2^{-/-}$ mice demonstrated normal commissural plate development demonstrating that commissural axon crossing of the midline does not influence commissural plate domain size *per se*. Thus, altered commissural plate patterning in other mutants such as $Emx2^{-/-}$ and $Nfia^{-/-}$ may provide an underlying cause for their commissural defects.

The mRNA of the morphogen FGF8 has been described as being notably expressed in the early rostral patterning center (Borello et al., 2008; Cholfin and Rubenstein, 2008) with ectopic expression of *Fgf8* being reported to affect the expression of the midline patterning genes *Zic2* and *Lhx2* (Hayhurst et al., 2008; Okada et al., 2008), of which *Lhx2* is postulated to coordinate forebrain development together with *Six3* (Ando et al., 2005). Moreover, misexpression of both *Zic2* and *Six3* in humans is associated with holoprosencephaly (HPE) (Brown et al., 1998; Wallis et al., 1999; Brown et al., 2001; Rosenfeld et al., 2010). In addition to these candidates, a comparative genomic hybridization of individuals with HPE recently identified a deletion in *FGF8* (Rosenfeld et al., 2010). However, except for a few expression studies (Yaylaoglu et al., 2005; Smith et al., 2006), the role of *Fgf8* in commissural plate development has not been investigated. Here, we found that *Fgf8* mRNA expression is found predominantly at the border of the MC and SA domains of the commissural plate, and consequently we found that loss of *Fgf8* in this region particularly affects the MC_2 and SA_1 regions, resulting in loss of the septum and failure of CC and HC crossing. This tissue loss is consistent with reports that *Fgf8* is required to maintain cell survival (Storm et al., 2006). In the absence of this tissue, re-specification of the tissue did not occur as the conditional *Fgf8* knockouts retained the relative dorso-ventral expression of the four commissural plate patterning genes. The AC did form in these mutants, supporting the hypothesis that the SA_2 is a separate domain of the commissural plate, which is not dominantly regulated by dorsal FGF8 expression within the *Emx1*-expressing telencephalon. Despite roles for *Fgf8* regulation of *Zic2* (Hayhurst et al. 2008; Okada et al. 2008), knockout of *Fgf8* under these conditions did not eliminate ZIC2 and SIX3 expression from neighboring tissue. Part of the reason may be that *Zic2* and *Six3* expression arises earlier than that of *Emx1* (Oliver et al., 1995; Elms et al., 2004) and hence these genes may be expressed before Cre-loxP recombination of the *Fgf8* transcript. Alternatively, in the absence of Fgf8, another unknown genetic regulation pathway acts to maintain cell survival and expression of ZIC2 and SIX3. Finally, the SIX3 and ZIC2 expression domains lie

outside the *Fgf8*-maintained tissue that became ablated in the current study. These results demonstrate an absolute requirement for FGF8 in the development of the central (MC_2 and SA_1) regions of the commissural plate.

An interesting question is how commissural plate development relates to the earlier events of midline formation and holoprosencephaly. From the present and previous studies ZIC2, SIX3, FGF8 and FGFR1/R3 contribute to the generation of midline tissue followed by its subsequent differentiation into the four domains of the commissural plate (including the septum; Tole et al., 2006). Loss of function mutations in *ZIC2*, *SIX3*, and *FGF8* result in varying forms of HPE in mice and humans (Brown et al., 1998; Meyers et al., 1998; Wallis et al. 1999; Brown et al., 2001; Warr et al., 2008; Rosenfeld et al., 2010). Recent studies have elegantly elucidated regulatory mechanisms involving *Zic*, *Six3* and *Shh*, and how these might be involved in HPE (Geng et al., 2008; Jeong et al., 2008; Warr et al., 2008; Marchal et al., 2009; Sanek et al., 2009). Mutations in *Zic2* are thought to cause HPE during formation of the prechordal plate, prior to *Fgf8* or *Shh* expression (Warr et al., 2008). *Six3* mutations have been shown to decrease *Shh* expression (Geng et al., 2008; Jeong et al., 2008). While decreasing telencephalic *Shh*, *Zic2*, or both, diminishes *Fgf8* expression in the rostral patterning centre, which precedes commissural plate formation (Warr et al., 2008). There is also evidence to suggest that *Fgf8* expression is independent of *Shh* (Gutin et al., 2006). Given this data and the data presented here it is likely that these genes play roles in the patterning and formation of midline tissue in early stages of development and then also regulate the further differentiation of these regions into the commissural plate, allowing the formation of different commissural projections to occur in precise dorsovental regions of the midline. In addition, further cellular events such as midline fusion must occur in this region to allow crossing of the forebrain commissures. At present nothing is known about the molecules controlling midline fusion but it is possible that similar genes might be involved given that our *Emx1-cre;Fgf8*$^{flox/flox}$ mutants display some defects in midline fusion, but whether this is directly regulated by FGF8 is yet to be determined.

The mechanisms regulating commissure formation in the brain are complex and involve a large number of genes (reviewed in Paul et al., 2007). Such important developmental events are hypothesized to include fusion of the telencephalic midline, as well as later developmental events such axon guidance mechanisms (reviewed in Lindwall et al., 2007). Here, we demonstrate that patterning of the midline and specificity of the four domains of the commissural plate provide another mechanism by which forebrain commissural axon projections are regulated.

Supplementary Material

Refer to Web version on PubMed Central for supplementary material.

Acknowledgments

Funding Acknowledgements

RXM is a C.J. Martin Fellow and LJR is a Senior Research Fellow of the NHMRC, Australia. This work was funded by an NHMRC grant to LJR (456027), NIH grants to SM (AG 20012, EB 003543, ES 01266). VT was supported by DFG-Research Center for Molecular Physiology of the Brain and by DFG grant TA 303/4-1.

Other acknowledgements

The authors would like to thank Erica Little, John Baisden, Jane Ellis, Michael Piper, Charlotta Lindwall, Guy Barry, Sharon Mason, Manuela Schwark and Janette Thurley for technical advice and assistance. Thank you to Peter Gruss (Max Planck Society, Munich, Germany) for providing the *Emx2* mutant line, Gail Martin (UCSF, USA) and Mike Lewandoski (Frederick Cancer Research and Development Center, MD, USA) for providing the

FGF8$^{flox/flox}$ line, Shigeyoshi Itohara (Riken Brain Science Institute, Japan) for providing the Emx1^{Cre} line, and Giorgio Corte (Advanced Biotechnology Center, Genova, Italy) for the anti-EMX1 antibody.

References

Abbie AA. The origin of the corpus callosum and the fate of the structures related to it. J Comp Neurol. 1940; 70:9–40.

Alcamo EA, Chirivella L, Dautzenberg M, Dobreva G, Farinas I, Grosschedl R, McConnell SK. Satb2 regulates callosal projection neuron identity in the developing cerebral cortex. Neuron. 2008; 57:364–377. [PubMed: 18255030]

Ando H, Kobayashi M, Tsubokawa T, Uyemura K, Furuta T, Okamoto H. Lhx2 mediates the activity of Six3 in zebrafish forebrain growth. Dev Biol. 2005; 287:456–468. [PubMed: 16226737]

Barry G, Piper M, Lindwall C, Moldrich R, Mason S, Little E, Sarkar A, Tole S, Gronostajski RM, Richards LJ. Specific glial populations regulate hippocampal morphogenesis. J Neurosci. 2008; 28:12328–12340. [PubMed: 19020026]

Bishop KM, Goudreau G, O'Leary DD. Regulation of area identity in the mammalian neocortex by Emx2 and Pax6. Science. 2000; 288:344–349. [PubMed: 10764649]

Boncinelli E, Gulisano M, Broccoli V. Emx and Otx homeobox genes in the developing mouse brain. J Neurobiol. 1993; 24:1356–1366. [PubMed: 7901323]

Briata P, Di Blas E, Gulisano M, Mallamaci A, Iannone R, Boncinelli E, Corte G. EMX1 homeoprotein is expressed in cell nuclei of the developing cerebral cortex and in the axons of the olfactory sensory neurons. Mech Dev. 1996; 57:169–180. [PubMed: 8843394]

Britanova O, Depew MJ, Schwark M, Thomas BL, Miletich I, Sharpe P, Tarabykin V. Satb2 haploinsufficiency phenocopies 2q32-q33 deletions, whereas loss suggests a fundamental role in the coordination of jaw development. Am J Hum Genet. 2006; 79:668–678. [PubMed: 16960803]

Britanova O, de Juan Romero C, Cheung A, Kwan KY, Schwark M, Gyorgy A, Vogel T, Akopov S, Mitkovski M, Agoston D, Sestan N, Molnar Z, Tarabykin V. Satb2 is a postmitotic determinant for upper-layer neuron specification in the neocortex. Neuron. 2008; 57:378–392. [PubMed: 18255031]

Brown LY, Kottmann AH, Brown S. Immunolocalization of Zic2 expression in the developing mouse forebrain. Gene Expr Patterns. 2003; 3:361–367. [PubMed: 12799086]

Brown LY, Odent S, David V, Blayau M, Dubourg C, Apacik C, Delgado MA, Hall BD, Reynolds JF, Sommer A, Wieczorek D, Brown SA, Muenke M. Holoprosencephaly due to mutations in ZIC2: alanine tract expansion mutations may be caused by parental somatic recombination. Hum Mol Genet. 2001; 10:791–796. [PubMed: 11285244]

Brown SA, Warburton D, Brown LY, Yu CY, Roeder ER, Stengel-Rutkowski S, Hennekam RC, Muenke M. Holoprosencephaly due to mutations in ZIC2, a homologue of Drosophila odd-paired. Nat Genet. 1998; 20:180–183. [PubMed: 9771712]

Campbell K. Dorsal-ventral patterning in the mammalian telencephalon. Curr Opin Neurobiol. 2003; 13:50–56. [PubMed: 12593982]

Cholfin JA, Rubenstein JL. Frontal cortex subdivision patterning is coordinately regulated by Fgf8, Fgf17, and Emx2. J Comp Neurol. 2008; 509:144–155. [PubMed: 18459137]

Crossley PH, Martin GR. The mouse Fgf8 gene encodes a family of polypeptides and is expressed in regions that direct outgrowth and patterning in the developing embryo. Development. 1995; 121:439–451. [PubMed: 7768185]

Elms P, Scurry A, Davies J, Willoughby C, Hacker T, Bogani D, Arkell R. Overlapping and distinct expression domains of Zic2 and Zic3 during mouse gastrulation. Gene Expr Patterns. 2004; 4:505–511. [PubMed: 15261827]

Geng X, Speirs C, Lagutin O, Inbal A, Liu W, Solnica-Krezel L, Jeong Y, Epstein DJ, Oliver G. Haploinsufficiency of Six3 fails to activate Sonic hedgehog expression in the ventral forebrain and causes holoprosencephaly. Dev Cell. 2008; 15:236–47. [PubMed: 18694563]

Gloor P, Salanova V, Olivier A, Quesney LF. The human dorsal hippocampal commissure. An anatomically identifiable and functional pathway. Brain. 1993; 116:1249–1273. [PubMed: 8221057]

Gutin G, Fernandes M, Palazzolo L, Paek H, Yu K, Ornitz DM, McConnell SK, Hébert JM. FGF signalling generates ventral telencephalic cells independently of SHH. Development. 2006; 133(15):2937–46. [PubMed: 16818446]

Gyorgy AB, Szemes M, de Juan Romero C, Tarabykin V, Agoston DV. SATB2 interacts with chromatin-remodeling molecules in differentiating cortical neurons. Eur J Neurosci. 2008; 27:865–873. [PubMed: 18333962]

Hanbury R, Ling ZD, Wuu J, Kordower JH. GFAP knockout mice have increased levels of GDNF that protect striatal neurons from metabolic and excitotoxic insults. J Comp Neurol. 2003; 461(3):307–316. [PubMed: 12746870]

Hayhurst M, Gore BB, Tessier-Lavigne M, McConnell SK. Ongoing sonic hedgehog signaling is required for dorsal midline formation in the developing forebrain. Dev Neurobiol. 2008; 68:83–100. [PubMed: 17948241]

Hebert JM. Unraveling the molecular pathways that regulate early telencephalon development. Curr Top Dev Biol. 2005; 69:17–37. [PubMed: 16243595]

Hines RJ, Paul LK, Brown WS. Spatial attention in agenesis of the corpus callosum: shifting attention between visual fields. Neuropsychologia. 2002; 40:1804–1814. [PubMed: 12062892]

His W. Die Entwicklung des menschlichen Rautenhirns vom Ende des ersten bis zum Beginn des dritten Monats: I. Verlangertes Mark. Abhandlungen der Mathematisch-Physischen Klasse der Koniglich-Sachsischen Gesellschaft der Wissenschaften XV. 1889

Hochstetter, F. Beitrage zur Entwicklungsgeschichte des menschlichen Gehirns. Vienna: Deuticke; 1929. II Teil 3. Lieferung. Die Entwicklung des Mittel- und Rautenhirns; p. 170

Iwasato T, Nomura R, Ando R, Ikeda T, Tanaka M, Itohara S. Dorsal telencephalon-specific expression of Cre recombinase in PAC transgenic mice. Genesis. 2004; 38:130–138. [PubMed: 15048810]

Jeong Y, Leskow FC, El-Jaick K, Roessler E, Muenke M, Yocum A, Dubourg C, Li X, Geng X, Oliver G, Epstein DJ. Regulation of a remote Shh forebrain enhancer by the Six3 homeoprotein. Nat Genet. 2008; 40:1348–53. [PubMed: 18836447]

Kawauchi S, Shou J, Santos R, Hebert JM, McConnell SK, Mason I, Calof AL. Fgf8 expression defines a morphogenetic center required for olfactory neurogenesis and nasal cavity development in the mouse. Development. 2005; 132:5211–23. [PubMed: 16267092]

Lavado A, Lagutin OV, Oliver G. Six3 inactivation causes progressive caudalization and aberrant patterning of the mammalian diencephalon. Development. 2008; 135:441–450. [PubMed: 18094027]

Mallamaci A, Muzio L, Chan CH, Parnavelas J, Boncinelli E. Area identity shifts in the early cerebral cortex of Emx2−/− mutant mice. Nat Neurosci. 2000; 3:679–686. [PubMed: 10862700]

Mao X, Fujiwara Y, Chapdelaine A, Yang H, Orkin SH. Activation of EGFP expression by Cre-mediated excision in a new ROSA26 reporter mouse strain. Blood. 2001; 97:324–326. [PubMed: 11133778]

Marchal L, Luxardi G, Thomé V, Kodjabachian L. BMP inhibition initiates neural induction via FGF signaling and Zic genes. Proc Natl Acad Sci U S A. 2009; 106:17437–17442. [PubMed: 19805078]

Maruoka Y, Ohbayashi N, Hoshikawa M, Itoh N, Hogan BL, Furuta Y. Comparison of the expression of three highly related genes, Fgf8, Fgf17 and Fgf18, in the mouse embryo. Mech Dev. 1998; 74:175–177. [PubMed: 9651520]

Meyers EN, Lewandoski M, Martin GR. An Fgf8 mutant allelic series generated by Cre- and Flp-mediated recombination. Nat Genet. 1998; 18:136–141. [PubMed: 9462741]

Mihalkovics, VV. Entwicklungsgeschichte des Gehirns nach Untersuchungen an höheren Wirbelthieren und dem Menschen. Leipzig: Engelmann; 1877.

Mori S, van Zijl PC. A motion correction scheme by twin-echo navigation for diffusion-weighted magnetic resonance imaging with multiple RF echo acquisition. Magn Reson Med. 1998; 40:511–516. [PubMed: 9771567]

Nielsen T, Montplaisir J, Lassonde M. Sleep architecture in agenesis of the corpus callosum: laboratory assessment of four cases. J Sleep Res. 1992; 1:197–200. [PubMed: 10607051]

O'Leary DD, Sahara S. Genetic regulation of arealization of the neocortex. Curr Opin Neurobiol. 2008; 18:90–100. [PubMed: 18524571]

O'Leary DD, Chou SJ, Sahara S. Area patterning of the mammalian cortex. Neuron. 2007; 56:252–269. [PubMed: 17964244]

Ogura H, Aruga J, Mikoshiba K. Behavioral abnormalities of Zic1 and Zic2 mutant mice: implications as models for human neurological disorders. Behav Genet. 2001; 31:317–324. [PubMed: 11699604]

Okada T, Okumura Y, Motoyama J, Ogawa M. FGF8 signaling patterns the telencephalic midline by regulating putative key factors of midline development. Dev Biol. 2008; 320:92–101. [PubMed: 18547559]

Oliver G, Mailhos A, Wehr R, Copeland NG, Jenkins NA, Gruss P. Six3, a murine homologue of the sine oculis gene, demarcates the most anterior border of the developing neural plate and is expressed during eye development. Development. 1995; 121:4045–4055. [PubMed: 8575305]

Paul LK, Van Lancker-Sidtis D, Schieffer B, Dietrich R, Brown WS. Communicative deficits in agenesis of the corpus callosum: nonliteral language and affective prosody. Brain Lang. 2003; 85:313–324. [PubMed: 12735947]

Paul LK, Brown WS, Adolphs R, Tyszka JM, Richards LJ, Mukherjee P, Sherr EH. Agenesis of the corpus callosum: genetic, developmental and functional aspects of connectivity. Nat Rev Neurosci. 2007; 8:287–299. [PubMed: 17375041]

Pellegrini M, Mansouri A, Simeone A, Boncinelli E, Gruss P. Dentate gyrus formation requires Emx2. Development. 1996; 122:3893–3898. [PubMed: 9012509]

Piper M, Plachez C, Zalucki O, Fothergill T, Goudreau G, Erzurumlu R, Gu C, Richards LJ. Neuropilin 1-Sema signaling regulates crossing of cingulate pioneering axons during development of the corpus callosum. Cereb Cortex. 2009; 19(Suppl 1):i11–21. [PubMed: 19357391]

Plachez C, Lindwall C, Sunn N, Piper M, Moldrich RX, Campbell CE, Osinski JM, Gronostajski RM, Richards LJ. Nuclear factor I gene expression in the developing forebrain. J Comp Neurol. 2008; 508:385–401. [PubMed: 18335562]

Rakic P, Yakovlev PI. Development of the corpus callosum and cavum septi in man. J Comp Neurol. 1968; 132:45–72. [PubMed: 5293999]

Rash BG, Richards LJ. A role for cingulate pioneering axons in the development of the corpus callosum. J Comp Neurol. 2001; 434:147–157. [PubMed: 11331522]

Ren T, Zhang J, Plachez C, Mori S, Richards LJ. Diffusion tensor magnetic resonance imaging and tract-tracing analysis of Probst bundle structure in Netrin1- and DCC-deficient mice. J Neurosci. 2007; 27:10345–10349. [PubMed: 17898206]

Richards LJ, Plachez C, Ren T. Mechanisms regulating the development of the corpus callosum and its agenesis in mouse and human. Clin Genet. 2004; 66:276–289. [PubMed: 15355427]

Rosenfeld JA, Ballif BC, Martin DM, Aylsworth AS, Bejjani BA, Torchia BS, Shaffer LG. Clinical characterization of individuals with deletions of genes in holoprosencephaly pathways by aCGH refines the phenotypic spectrum of HPE. Hum Genet. 2010 Published online 12 January, 2010.

Rubenstein JL, Shimamura K, Martinez S, Puelles L. Regionalization of the prosencephalic neural plate. Annu Rev Neurosci. 1998; 21:445–477. [PubMed: 9530503]

Sanek NA, Taylor AA, Nyholm MK, Grinblat Y. Zebrafish zic2a patterns the forebrain through modulation of Hedgehog-activated gene expression. Development. 2009; 136:3791–800. [PubMed: 19855021]

Schreyer DJ, Skene JH. Fate of GAP-43 in ascending spinal axons of DRG neurons after peripheral nerve injury: delayed accumulation and correlation with regenerative potential. J Neurosci. 1991; 11:3738–3751. [PubMed: 1836017]

Shen Y, Mani S, Donovan SL, Schwob JE, Meiri KF. Growth-associated protein-43 is required for commissural axon guidance in the developing vertebrate nervous system. J Neurosci. 2002; 22:239–247. [PubMed: 11756507]

Shu T, Butz KG, Plachez C, Gronostajski RM, Richards LJ. Abnormal development of forebrain midline glia and commissural projections in Nfia knock-out mice. J Neurosci. 2003; 23:203–212. [PubMed: 12514217]

Smith KM, Ohkubo Y, Maragnoli ME, Rasin MR, Schwartz ML, Sestan N, Vaccarino FM. Midline radial glia translocation and corpus callosum formation require FGF signaling. Nat Neurosci. 2006; 9:787–797. [PubMed: 16715082]

Steele-Perkins G, Plachez C, Butz KG, Yang G, Bachurski CJ, Kinsman SL, Litwack ED, Richards LJ, Gronostajski RM. The transcription factor gene Nfib is essential for both lung maturation and brain development. Mol Cell Biol. 2005; 25:685–698. [PubMed: 15632069]

Takahashi H, Liu FC. Genetic patterning of the mammalian telencephalon by morphogenetic molecules and transcription factors. Birth Defects Res C Embryo Today. 2006; 78:256–266. [PubMed: 17061260]

Wallis DE, Roessler E, Hehr U, Nanni L, Wiltshire T, Richieri-Costa A, Gillessen-Kaesbach G, Zackai EH, Rommens J, Muenke M. Mutations in the homeodomain of the human SIX3 gene cause holoprosencephaly. Nat Genet. 1999; 22(2):196–8. [PubMed: 10369266]

Warr N, Powles-Glover N, Chappell A, Robson J, Norris D, Arkell RM. Zic2-associated holoprosencephaly is caused by a transient defect in the organizer region during gastrulation. Hum Mol Genet. 2008; 17(19):2986–96. [PubMed: 18617531]

Yaylaoglu MB, Titmus A, Visel A, Alvarez-Bolado G, Thaller C, Eichele G. Comprehensive expression atlas of fibroblast growth factors and their receptors generated by a novel robotic in situ hybridization platform. Dev Dyn. 2005; 234:371–386. [PubMed: 16123981]

Yoshida M, Suda Y, Matsuo I, Miyamoto N, Takeda N, Kuratani S, Aizawa S. Emx1 and Emx2 functions in development of dorsal telencephalon. Development. 1997; 124:101–111. [PubMed: 9006071]

Zuckerkandl E. Zur Entwickelung des Balkens und des Gewolbes. Sitz-Ber dk Akad d Wissensch Math-Naturwissensch. 1901; 110:233–307.

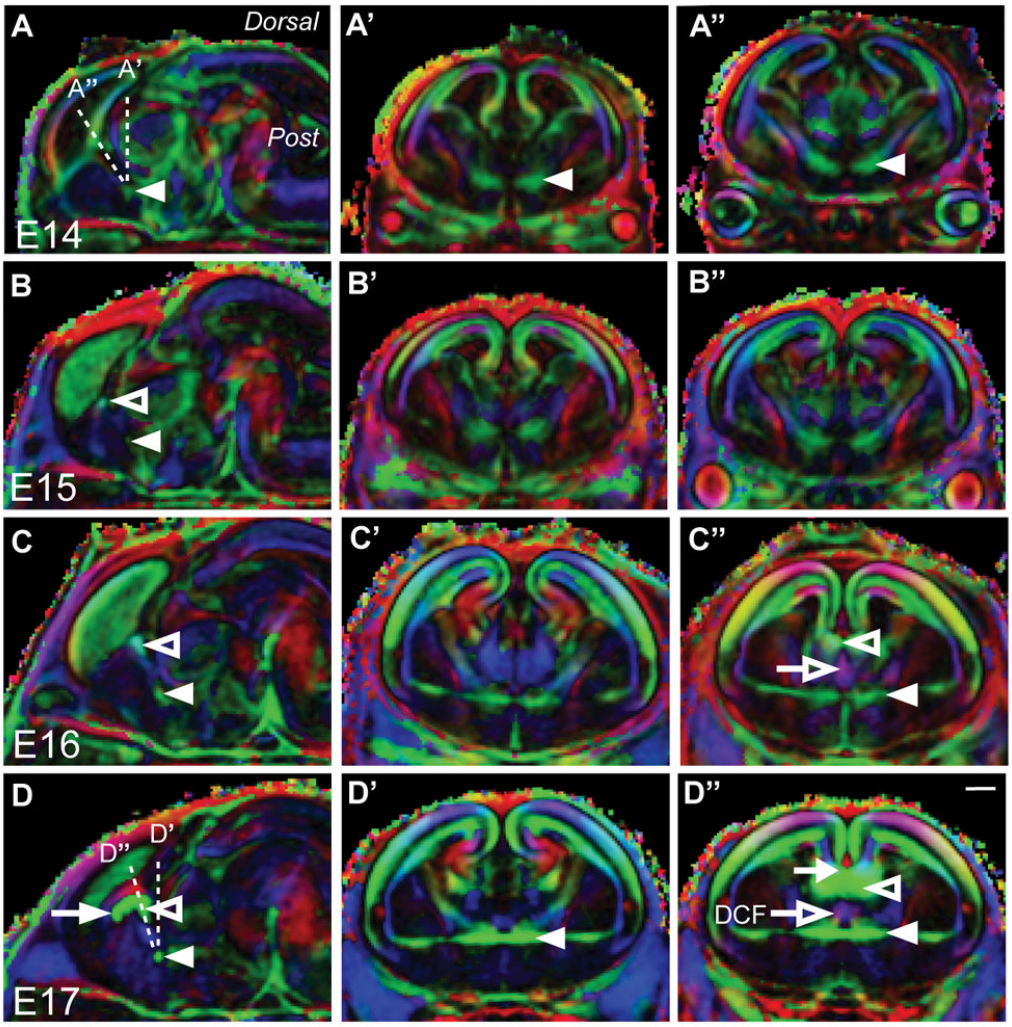

Figure 1.

DTMRI analysis of the developing mouse commissural plate shows the midline crossing of the commissures occurs at an oblique coronal angle. ***A-D″,*** Color maps generated from fractional anisotropy values and primary eigenvectors. Diffusion directions: green, medial to lateral; blue, anterior to posterior; red, dorsal to ventral. The CC, HC and AC are indicated by the arrow, open arrowhead and closed arrowhead, respectively. In ***A***, the difference in sectioning angle between the coronal plane (***A′***) and the oblique coronal plane (***A″***) can be appreciated by the dashed lines. Development of the commissures can be observed in the sagittal plane (***A, B, C, D***). The AC can be visualized by DTMRI proximal to the midline at E14 (***A***). ***B*:** By E15, the HC can also be visualized. At E16, the AC and HC have grown (***C***). ***D*:** By E17 all forebrain commissures have crossed the midline. The medial to lateral development of these commissures cannot be appreciated simultaneously in the traditional coronal plane alone (***A′, B′, C′, D′***). However, in an oblique coronal plane, determined from the sagittal images, all three commissures can be observed (***A″, B″, C″, D″***). For example, the CC (closed arrow) and HC (open arrowhead) are not present in the coronal plane at E17 (***D′***), but appear together in the oblique coronal plane (***D″***). In both ***C″*** and ***D″*** the descending columns of the fornix (DCF) can be seen in purple (open arrow), dorsal to the AC (closed arrowhead). Scale bar = 200 μm.

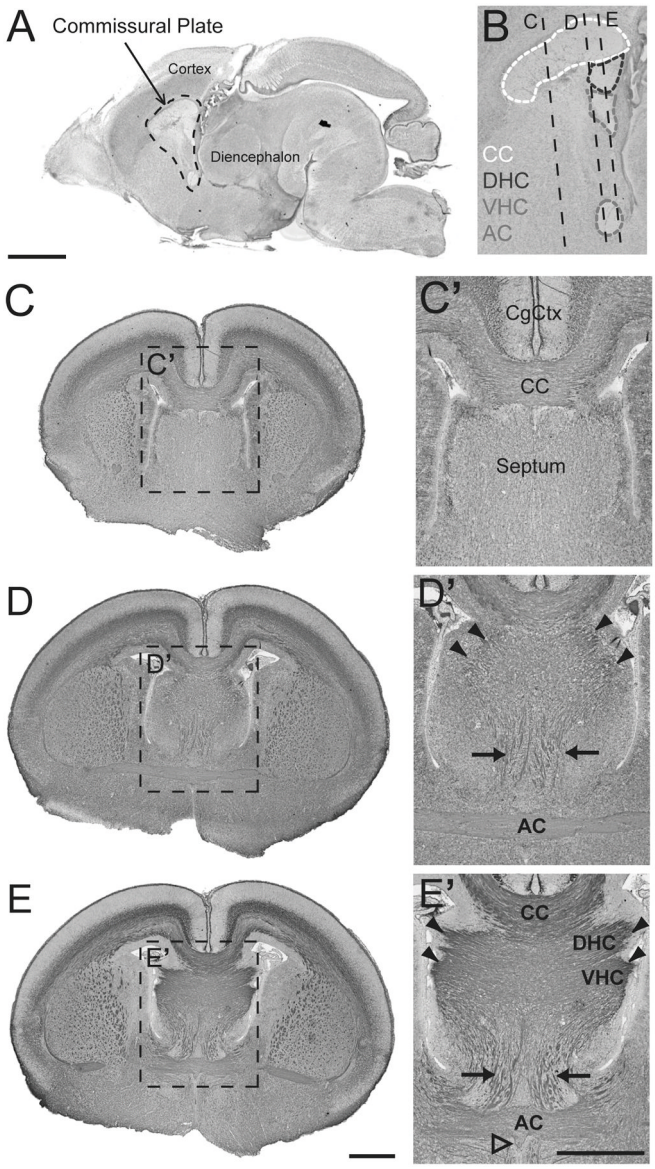

Figure 2.

Four distinct fiber tracts emerge within the mouse commissural plate by E17. ***A*:** Representative photomicrograph of a mid-sagittal section of E17 C57Bl/6 brain stained with hematoxylin. ***B*:** A 2.5× enlargement of the commissural plate in ***A***. Axon tracts of the corpus callosum (CC, green), dorsal hippocampal commissure (DHC, blue), ventral hippocampal commissure (VHC, red) and anterior commissure (AC, pale blue) are outlined. The putative commissural plate has been outlined in black (***A***). Dashed vertical lines indicate the oblique coronal angle used to obtain sections in **C-E**. ***C-E*:** Representative rostral to caudal sections of the commissural plate at E17, immunolabeled with anti-GAP43 (brown) for growing neuronal processes and counterstained with hematoxylin (blue). ***C′, D′, E ′*:** Enlargements of highlighted regions in C-E. ***C′*:** In a rostral plane of the commissural plate, the CC crosses the midline at the boundary between the cingulate cortex (CgCtx) and the septum. CC crossing at this boundary continues caudally. ***D′*:** In addition to the CC, ipsilateral descending columns of the fornix (arrows) and dorsal and ventral segments of the HC begin to emerge (arrowheads). ***E′*:** At the most caudal extent of the commissural plate

all four forebrain commissures cross the midline within the same oblique plane. From dorsal to ventral these are the CC, DHC (arrowheads), VHC (arrowheads) and AC. Also seen in ***E′*** is the caudal extent of the descending columns of the fornix (arrows) projecting ventrally between the VHC and the AC. Fibers of the AC are in direct contact with the ventricular zone of the third ventricle at the midline (open arrowhead). Scale bar in *A* = 1 mm, scale bars in *C*-*E′* = 500 μm.

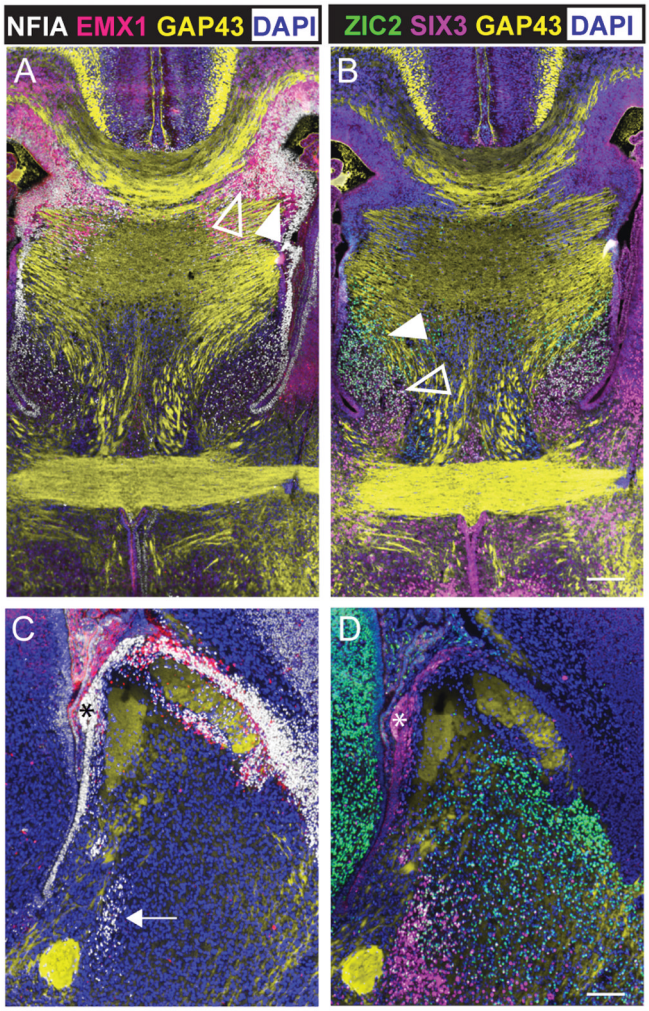

Figure 3.

Molecular delineation of the mouse commissural plate at E17 reveals four subdomains. Fluorescence immunohistochemistry of the dorsal telencephalic markers NFIA (closed arrowhead, ***A***) and EMX1 (open arrowhead, ***A***) at E17 in the oblique coronal plane and sagittal plane, where two (5μm think) adjacent sections have been overlaid (***A, C***). The ventral telencephalic markers SIX3 (open arrowhead) and ZIC2 (closed arrowhead) are expressed in the same sections (***B, D***). GAP43 labeling is shown in yellow to delineate the commissural axons. DAPI counterstain is shown in blue. While both NFIA and EMX1 encircle the rostral to caudal extent of the CC and surround the DHC, only NFIA expression spans the commissural plate ventrally to end rostral and dorsal of the AC (arrow). From the VHC towards the AC, the ventral markers ZIC2 and SIX3 are expressed in opposing gradients. ZIC2 is predominantly expressed around the fornix, while SIX3 is predominantly expressed around the AC. Laterally, ZIC2 is expressed within the septum, bounded by the lateral ventricles. However, SIX3 is expressed along the mediolateral extent of the AC. Immunoreactivity is also present in the choroid plexus and the epithelium of the rostral wall of the third ventricle (asterisks in ***C*** and ***D***). These features are not considered part of the commissural plate. From these expression patterns dorsal domains (MC) and ventral domains (SA) are characterized as follows: MC or MC_1, $NFIA^+$ and $EMX1^+$; MC_2 $NFIA^+$ and $ZIC2^+$; SA_1, $NFIA^+$ and $ZIC2^+$ and $SIX3^+$; SA_2, $SIX3^+$. Scale bars: *A-B* = 200 μm, *C-D* = 150 μm.

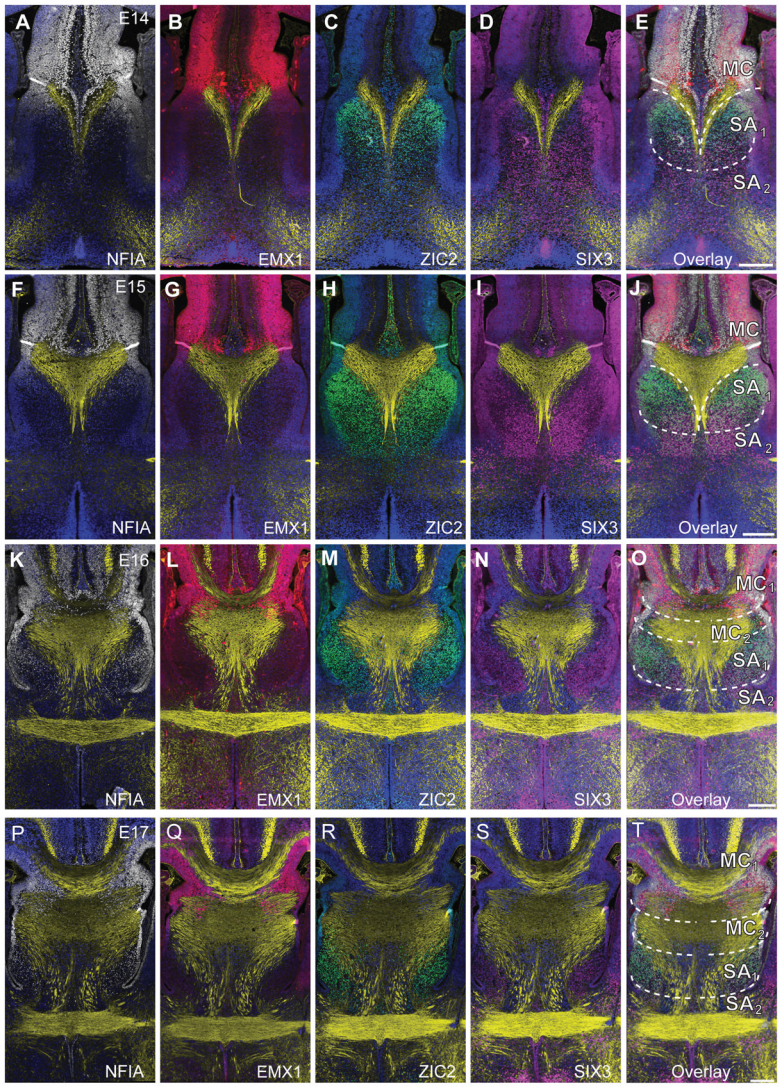

Figure 4.

Molecular patterning and morphology of the developing mouse commissural plate demonstrates the emergence of the four subdomains. Fluorescence immunohistochemistry for the markers NFIA (white), EMX1 (red), SIX3 (magenta) and ZIC2 (green) throughout the developmental oblique coronal plane of the commissural plate in mouse embryos at E14 (***A-E***), E15 (***F-J***), E16 (***K-O***) and E17 (***P-T***). GAP43 staining is shown in yellow. DAPI counterstain is shown in blue. An overlay of this molecular patterning is shown with boundaries indicated by dashed lines, defining dorsal domains (MC) and ventral domains (SA), characterized as follows: MC or MC_1, $NFIA^+$ and $EMX1^+$; MC_2 $NFIA^+$ and $ZIC2^+$; SA_1, $NFIA^+$ and $ZIC2^+$ and $SIX3^+$; SA_2, $SIX3^+$. Scale bar = 200 μm.

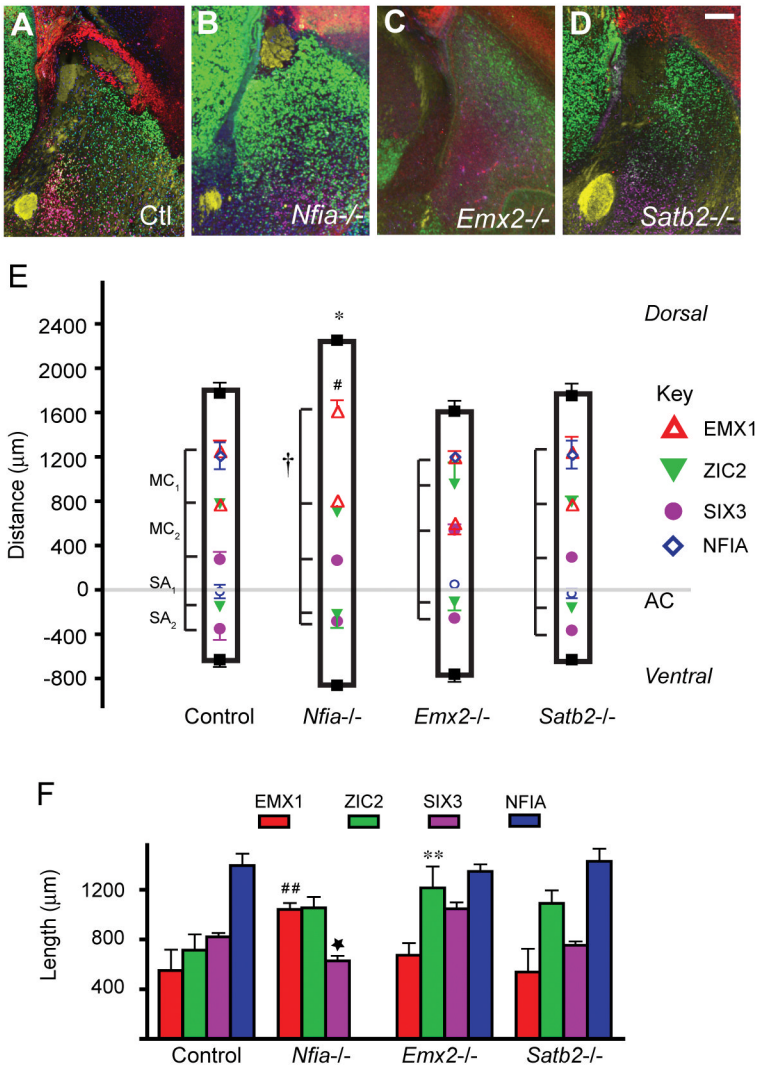

Figure 5.

Commissural plate domains are disrupted in *Emx2*$^{-/-}$ and *Nfia*$^{-/-}$, but not *Satb2*$^{-/-}$mice. Fluorescence immunohistochemistry in the sagittal plane for GAP43 (yellow), EMX1 (red), ZIC2 (green) and SIX3 (magenta) reveals the anatomical and molecular features of the commissural plate in wildtype (***A***), *Nfia*$^{-/-}$ (***B***), *Emx2*$^{-/-}$ (***C***), and *Satb2*$^{-/-}$ mice (***D***). NFIA immunoreactivity is not shown here because measurements were taken from additional sequential, but not adjacent, sagittal sections that did not allow overlay. Loss of the CC is seen in *Nfia*$^{-/-}$ mice (***B***), where DHC and VHC dysgenesis is also apparent. Agenesis of the CC and HC is apparent in *Emx2*$^{-/-}$ (***C***) and *Satb2*$^{-/-}$ mice (***D***). The AC is enlarged in *Satb2*$^{-/-}$ mice (***D***). ***E*:** Quantification of the commissural plate molecular boundaries as dorsoventral distances from the center of the AC. The MC, SA_1 and SA_2 domains are indicated to the left of the bars. Key to symbols: squares, dorsal and ventral surfaces of the brain; open upward triangles, EMX1; closed downward triangles, ZIC2; closed circles, SIX3. Wildtype littermates served as controls for the mutant mice. * $p < 0.05$ compared to the dorsal height of control. $^{\#}$ $p < 0.05$ compared to the dorsal extent of EMX1 expression of control. † $p < 0.05$ compared to MC of control. ***F*:** Molecular domain lengths for each of the mouse strains. Domain length calculations were based on linear distance along the oblique angle of the commissural plate, as demonstrated in Supp. Fig. 2. $^{\#\#}$ $p < 0.05$ compared to

EMX1 of control. ** $p < 0.05$ compared to ZIC2 of control. Star = $p < 0.05$ compared to SIX3 of control. Scale bar = 150 μm.

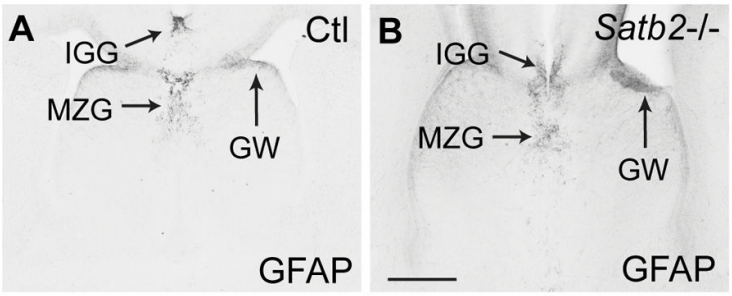

Figure 6.

Glial populations form normally in *Satb2* knockout mice. Glial populations within the commissural plate at E17 include the indusium griseum glia (IGG) at the dorsal limit of the MC_1, the glial wedge (GW) at the ventral limit of the MC_1, and the midline zipper glia (MZG) also at the boundary of the MC_1 and MC_2. A small population of glia surrounds the AC at the boundary of the SA_1 and SA_2. These populations can be seen in the wildtype CoP in ***A***. In *Satb2*$^{-/-}$ mice all glial populations are present and appear normal (***B)***. The indusium griseum glia and midline zipper glia are usually split by the formation of the corpus callosum but this does not occur due to the absence of the corpus callosum in *Satb2*$^{-/-}$ mice. Scale bar = 400 μm.

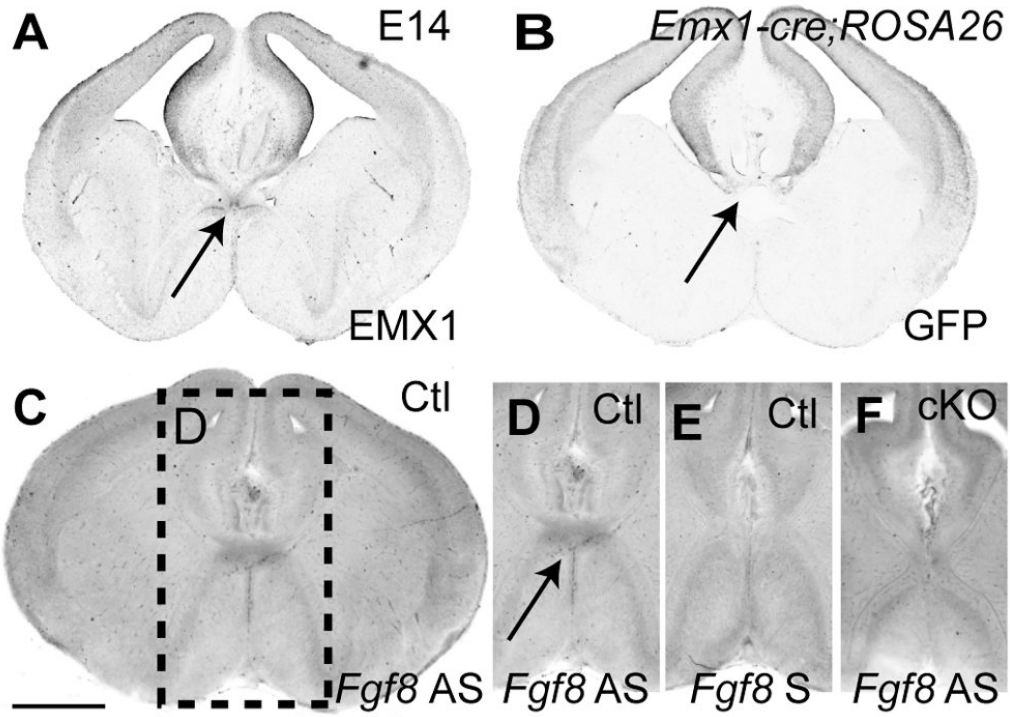

Figure 7.

Absence of *Fgf8* at the commissural plate in the *Emx1-cre;Fgf8*$^{flox/flox}$ mice. ***A*:** Immunohistochemistry shows EMX1 expression in the pallium and medial telencephalon extending ventrally to the lamina terminalis. ***B*:** Emx1-cre and ROSA26$^{flox/flox}$ mice were crossed to obtain a green fluorescent protein (GFP) profile of the extent of *Emx1*-cre recombinase activity. Immunohistochemistry for GFP at E14 reveals recombinase activity in the pallium. In particular, recombinase activity occurs around the dorsal part of the lamina terminalis (arrow). ***C*** and ***D*:** *In situ* hybridization in *Emx1*$^{+/+}$*;Fgf8*$^{flox/flox}$ (Ctl) mice demonstrates that *Fgf8* is expressed in the commissural plate at E14 at the border of the MC and SA domains. By contrast, sense *in situ* hybridization in control mice (***E***) and antisense *in situ* hybridization in *Emx1-cre;Fgf8*$^{flox/flox}$ (cKO) mice (***F***) reveal no *Fgf8* expression. Due to the restricted overlay of expression domains, the telencephalon develops without major deficit until E14. Scale bar = 400 μm.

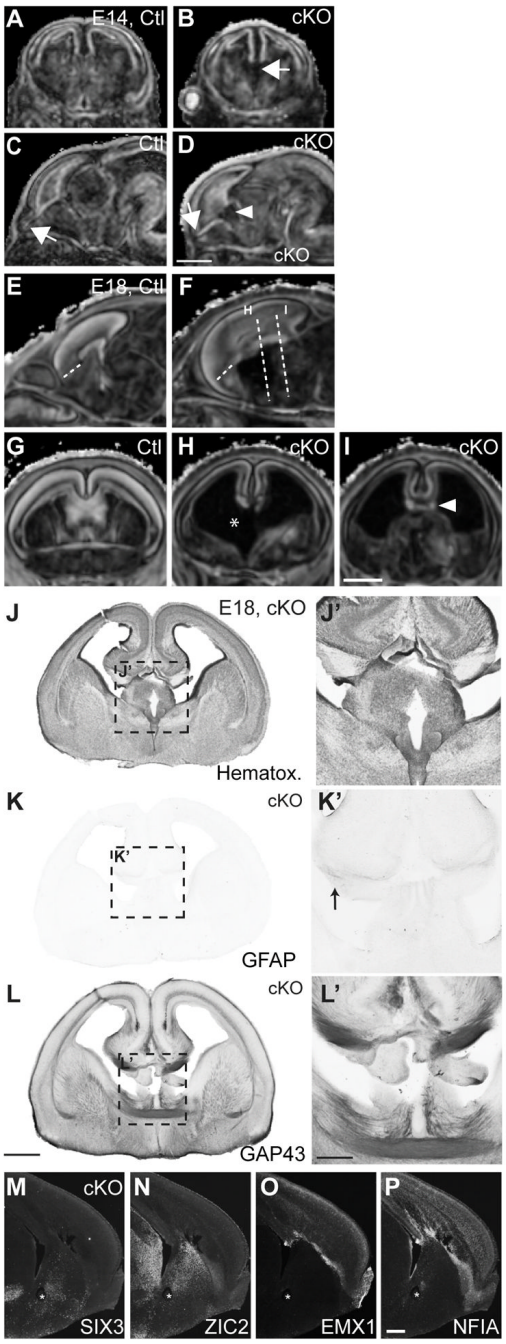

Figure 8.

Agenesis of the commissural plate in *Fgf8* hypomorphs. Fractional anisotropy images of the *Emx1-cre;Fgf8*$^{flox/flox}$ (cKO) heads and littermate controls (Ctl) at E14 (***A-D***) and E18 (***E-I***) where the intensity of white features indicates tissue and white matter tracts, while black indicates fluid spaces such as ventricles. At E14, cKO mutants show absence of the commissural plate (arrowhead in ***D***), failure of midline fusion (arrow in ***B***) and hypoplasia of the olfactory bulbs (arrows in ***C*** and ***D***). At E18, further dysmorphologies are seen, including agenesis of the corpus callosum and hippocampal commissure (arrowhead, ***I***), displacement of the corticoseptal boundary in the anterior telencephalon (compare hatched lines in ***E*** and ***F***) and communication of the lateral ventricles can be seen (asterisk, ***H***). ***H***

and ***I*** correspond to hatched lines in ***F***. ***J-K***: Hematoxylin stain shows the architecture of the brain at the coronal plane approximate to ***I***. Hypoplasia of the neocortex can be seen in ***J***, and hypoplasia of the commissural plate is evident ***J′***. ***K-K′*:** All but few glia are eliminated following conditional knockout of *Fgf8* as shown by immunohistochemistry for GFAP at the coronal plane approximate to ***I***. A few fimbrial glia are indicated by the arrow in ***K′***. ***L-L′*:** While axons of the fimbria stained with anti-GAP43 and the AC are present in cKO mice, midline crossing only occurs for the AC. ***M-P*:** Expression of the commissural plate markers are disrupted, but not eliminated by conditional knockout of *Fgf8*, as shown by immunohistochemistry for commissural plate markers EMX1, NFIA, ZIC2 and SIX3 in the mid-sagittal plane of E17 cKO mice. Scale bars: *A-D* = 600 μm; *E-I* = 700 μm; *J*, *L*, *N* = 1 mm; *K*, *M*, *O* = 500 μm; *P-S* = 300 μm.

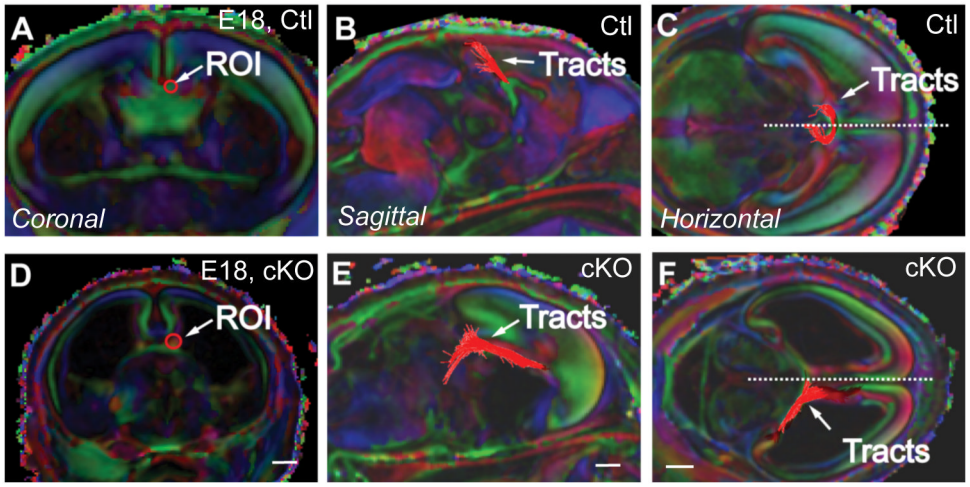

Figure 9.

DTMRI tractography in E18 brains of *Emx1-cre;Fgf8*$^{flox/flox}$ mice (cKO). From a region of interest (ROI) in the corpus callosum (***A-F***), tractography in mutants shows profound misprojections that fail to cross the midline (hatched line) compared to wildtype littermates (Ctl). Probst bundles are apparent from an ROI in the corpus callosum (***E*** and ***F***). Tractography was performed with DTI-Studio (tracking thresholds: angle <70 degrees, FA>0.3). Scale bar A, D = 0.7 mm; B, E = 0.8 mm; C, F = 1 mm.

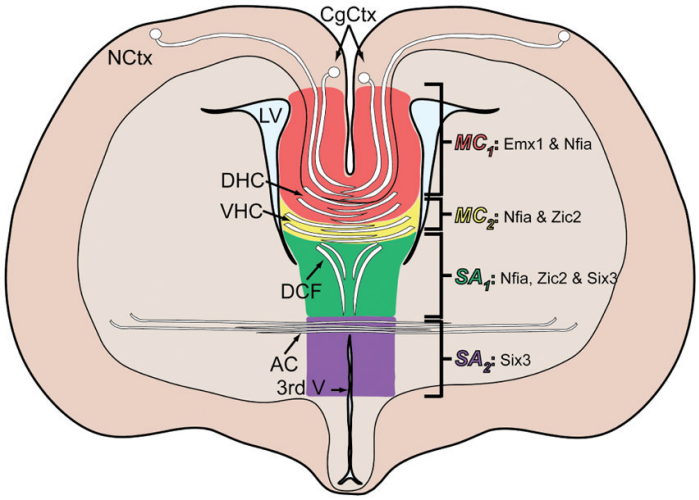

Figure 10.

Schematic of the commissural plate at an oblique coronal angle showing the commissures and their associated molecular domains. Abbreviations: 3rd V, third ventricle; CgCtx, cingulate cortex; LV, lateral ventricle; NCtx, neocortex.

Table 1

Mouse strains used.

Mouse strain	Transgene	Reference
Emx2	250 bp fragment deletion in the 5′ part of the homeobox with Neo insert	Pellegrini et al., 1996
Nfia	700 bp deletion including all but 9 bp of exon 2, with LacZ/Neo insert	Steele-Perkins et al., 2005
$Fgf8^{flox}$	loxP sites were inserted in the intron upstream of exon 2 and another in the 3′-UTR allowing excision of exons 2 and 3	Meyers et al., 1998
$Emx1^{cre}$	A nuclear localization signal-Cre-poly (A) signal was inserted, in the sense orientation, immediately 5′ to the *Emx1* translational initiation site (ATG) into a PAC-Emx1 clone	Iwasato et al., 2004
Satb2	Deletion of exon 2 and Cre insertion (null allele)	Britanova et al., 2006
ROSA26-$eGFP^{flox}$	a *loxP*-flanked STOP fragment lies between the eGFP gene and the *Gt(ROSA)26Sor* promoter	Mao et al., 2001

Table 2

Primary antibodies used in immunohistochemistry analysis

Antibody	Host, isotype	Source, Cat. No.	Antigen	Protocol, dilution
NFIA	Rb, IgG	Active Motif, 39329	478-492aa of human NFIA	IHC-P, 1:1000
EMX1	Rb, serum	Gift:	h*Emx1* cDNA full length protein	IHC-P, 1:500; IHC- FrFl, 1:1000
SIX3	Gp, IgG	Rockland, 200-201-A26	270-289aa of mouse Six3	IHC-P, 1:200
ZIC2	Rb, serum	Brown et al., 2003	2–109aa peptide from h*Zic2* cDNA	IHC-P, 1:1000
GAP-43	Ms, Clone 9-1E12	Chemicon, MAB347	purified rat brain GAP-43	IHC-P, 1:100
GFAP	Rb, IgG	DAKO, Z0334	Bovine spinal cord isolate	IHC-FrFl, 1:30,000
GFP	Rb, IgG	Invitrogen, A11122	*A. victoria* isolate	IHC-FrFl, 1:1000

IHC-P, paraffin section immunohistochemistry; IHC-FrFl, vibratome-sectioned free-floating immunohistochemistry; Gp, guinea pig; Ms, mouse; Rb, rabbit.